Transition of flow past a couple of cylinders placed in a uniform flow

Jiro Mizushima∗ and Yoichi Ino

Department of Mechanical Engineering, Doshisha University, Kyotanabe, Kyoto 610-0321, Japan

E-mail: `jmizushi@mail.doshisha.ac.jp`∗

Abstract. Instability and transition of flow past a couple of circular cylinders arranged perpendicularly to the stream are investigated numerically. It is a steady symmetric flow that is realized at small Reynolds numbers, but the flow becomes unstable above a critical Reynolds number and exhibits various flow patterns. Although the resultant flow is expected to be oscillatory, an asymmetric oscillatory flow pattern was reported to appear due to the instability. The physical origin of the asymmetric oscillatory flow is explored in the present paper and identified as the instability due to a stationary disturbance. A steady asymmetric flow is found to arise from the instability in a very narrow region of the gap width between the two cylinders. We evaluate the region of the gap width in which the steady asymmetric flow is realized as well as the critical Reynolds number.

1. Introduction

Flow past two circular cylinders has been investigated in various areas of engineering and science. The configuration of the cylinders is classified into three arrangements: tandem, side–by–side and staggered. It is said that research on the flow past two tandem cylinders was motivated by an application to twin struts to support wings of airplane so that the drag and lift coefficients on the cylinders were the main concern of researchers. On the other hand, flow patterns have been focused in the research of flow past two cylinders in the side-by-side arrangement, where change of the flow pattern with an increase or decrease of the gap with between the two cylinders has been investigated in detail.

For the tandem arrangement of two cylinders, it is known that physical quantities such as the drag and lift coefficients and the Strouhal number show an abrupt change even when the gap spacing between the two cylinders is continuously changed[1]. The critical spacing is evaluated to be about 3.5 diameters, although the value scatters, depending mostly on the Reynolds number. The existence of the critical spacing was confirmed by Ishigai *et al.* in their experiment in the range of the Reynolds number of $1500 - 15000$[2]. They evaluated the critical spacing to be 3.8 diameters. The origin of the abrupt change in these physical quantities was investigated numerically by Mizushima and Suehiro, and clarified to come from a hysteretic structure of the bifurcation diagram of solution[3].

Researches on flow past two cylinders in the side–by–side arrangement have been performed at large Reynolds numbers ($Re = 10^3 \sim 10^4$) mostly in experiments, where the frequency in the wake behind the two cylinders was measured, and deflected flows through the gap between the cylinders were observed[2, 4]. Ishigai *et al.* attributed the appearance of the deflected flow to a
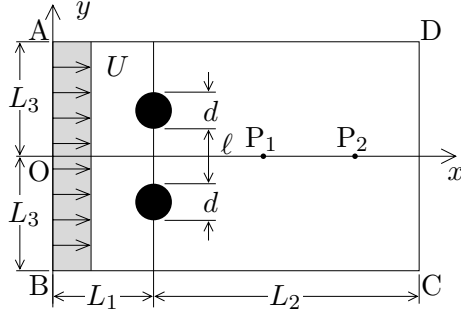
Figure 1. Configuration and co-ordinates.

Coanda effect, whereas Williamson denied it and proposed to apply the stability theory to this problem. Recently, Kang made numerical simulation for the flow at small Reynolds numbers such as $Re = 40 \sim 160$, and classified the flow into six flow patterns depending on the Reynolds number and the spacing between the two cylinders, in which the deflected oscillatory flow is confirmed[5].

In spite of many reports on the flow past two cylinders in the side–by–side arrangement, their attention was paid mostly to the flow patterns, and the origin of the flows or the mechanism to generate such flows has not been examined in detail. We investigate the transition of the flow by the numerical simulation and the stability analysis in the present paper. Our major objective is to explore the origin of various flow patterns, specifically the origin of the deflected oscillatory flow.

2. Mathematical formulation and boundary conditions

Consider the flow past two circular cylinders placed side–by–side in a uniform flow with velocity U as illustrated in Fig. 1. The two circular cylinders have the same diameter d, and the gap spacing between them is ℓ. We take x-axis in the direction of the uniform flow upstream and y-axis perpendicularly to it. Taking d and U as the representative length and velocity scales, we define the gap ratio Γ as $\Gamma \equiv \ell/d$ and the Reynolds number Re as $Re \equiv Ud/\nu$, respectively.

Assuming an incompressible two–dimensional flow field and employing the stream function $\psi(x, y, t)$ and the vorticity $\omega(x, y, t)$ formulation, we write the governing equations of the flow, i.e. the vorticity transport and Poisson equations, in nondimensional form as

$$\frac{\partial \omega}{\partial t} = \mathcal{N}(\psi, \omega) + \mathcal{M}\omega, \tag{1}$$

$$\omega = -\mathcal{M}\psi, \tag{2}$$

$$\mathcal{N}(\psi, \omega) \equiv \frac{\partial \psi}{\partial x}\frac{\partial \omega}{\partial y} - \frac{\partial \psi}{\partial y}\frac{\partial \omega}{\partial x}, \quad \mathcal{M} \equiv \frac{\partial^2}{\partial x^2} + \frac{\partial^2}{\partial y^2}.$$

Here, $\mathcal{M}$ is the two–dimensional Laplacian and $\mathcal{N}$ shows the nonlinear term.

The assumed infinitely extended flow field is approximated by the finite domain indicated by ABCD in Fig. 1. Uniform flow is assumed to come to the upstream boundary (AB). The outlet condition at the downstream boundary (CD) is approximated by the Sommerfeld radiation condition. The non-slip condition is applied on the surface of each circular cylinder. The condition on side boundaries (AD and BC) is also uniform flow.

3. Steady–state solution

At small Reynolds numbers, the flow is steady and symmetric with respect to the x-axis, i.e., the centerline through the midst of the gap between the two cylinders. The solution corresponding to the steady symmetric flow satisfies basic equations (1) and (2) under the boundary conditions, irrespectively of the value of the Reynolds number, although it becomes unstable above a critical value. This steady symmetric flow, say $(\bar{\psi}, \bar{\omega})$, is the main flow for the linear stability analysis. The main flow is obtained numerically by solving the steady–state vorticity transport equation:

$$\mathcal{N}(\bar{\psi}, \bar{\omega}) + \frac{1}{Re}\mathcal{M}\bar{\omega} = 0, \tag{3}$$

which is obtained by dropping the term including the time–derivative in Eq. (1), together with the Poisson equation:

$$\bar{\omega} = -\mathcal{M}\,\bar{\psi} \tag{4}$$

under the appropriate boundary conditions.

4. Linear stability analysis

The flow is steady and symmetric with respect to the centerline through the gap between the two cylinders (x-axis) at small Reynolds numbers. For a larger Reynolds number than the critical value Re_c, the steady symmetric flow is unstable to a disturbance and makes a transition to a periodic flow or an asymmetric steady flow. We consider a disturbance (ψ', ω') added to the main flow $(\bar{\psi}, \bar{\omega})$ and express the stream function and the vorticity as

$$\psi = \bar{\psi} + \psi', \quad \omega = \bar{\omega} + \omega', \tag{5}$$

respectively. Substituting these expressions into Eq. (1) and subtracting Eq. (3), we obtain a nonlinear disturbance equation for the vorticity disturbance ω' as

$$\frac{\partial \omega'}{\partial t} = \frac{1}{Re}\mathcal{M}\omega' + \mathcal{N}(\psi', \bar{\omega}) + \mathcal{N}(\bar{\psi}, \omega') + \mathcal{N}(\psi', \omega'). \tag{6}$$

Neglecting the nonlinear term of the disturbance (ψ', ω') in Eq. (6) and assuming the time dependence of the disturbance as $\psi' = \hat{\psi}(x, y)e^{\lambda t}$, $\omega' = \hat{\omega}(x, y)e^{\lambda t}$, we arrive at a linealized disturbance equation:

$$\lambda\hat{\omega} = \frac{1}{Re}\mathcal{M}\hat{\omega} + \mathcal{N}(\hat{\psi}, \bar{\omega}) + \mathcal{N}(\bar{\psi}, \hat{\omega}), \tag{7}$$

which is solved together with the Poisson equation for the disturbance:

$$\hat{\omega} = -\mathcal{M}\hat{\psi}. \tag{8}$$

Here, the coefficient λ is a complex linear growth rate of the disturbance, whose real and imaginary parts λ_r and λ_i, show the growth rate and the frequency (angular velocity) of the disturbance, respectively. The steady symmetric flow is unstable if λ_r is positive, or stable if λ_r is negative. Hence, the Reynolds number where $\lambda_r = 0$ gives the critical value Re_c.

The boundary condition for $(\hat{\psi}, \hat{\omega})$ on the upstream and side boundaries is given as $(\hat{\psi}, \hat{\omega}) = (0, 0)$. The outlet condition on the downstream boundary is the Sommerfeld radiation condition. The non-slip boundary condition is applied on the surface of each circular cylinder.
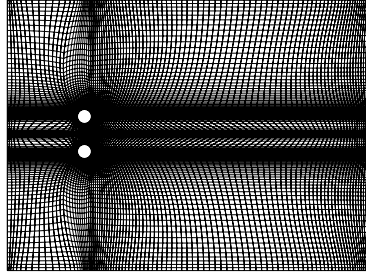
Figure 2. Computational grid. $\Gamma = 1.5$

.

5. Numerical method

We utilize two different numerical methods, one of which is numerical simulation of basic equations (1) and (2) under the boundary conditions and an appropriate initial condition and the other the linear stability analysis of the steady symmetric flow. In both the numerical calculation, the numerical domain is defined as $L_1 = 5d$, $L_2 = 20d$ and $L_3 = \ell/2 + 9d$, which must be large enough not to affect the results (see Fig. 1). A curvilinear numerical grid is generated to fit the circular cylinders, for which Poisson equations are solved and the technique proposed by Steger and Sorenson is used in order to cluster grid points near the surfaces of cylinders[6]. An example of the grid thus generated is shown in Fig. 2 for $\Gamma = 1.5$, whose total number of mesh points is 299×310; the minimum mesh size is $0.01d$ near the surfaces of the cylinders and the maximum size is $0.1d$ near the outlet and side boundaries.

In numerical simulation of dynamical equation (1), we use the forth–order Runge–Kutta method to approximate the time integration together with the second–order accuracy of central finite difference in space. Poisson equation (2) is solved by the successive over relaxation (SOR) method, in which the relaxation factor is mostly taken as $\epsilon = 1.5$, although other values are also taken depending on the value of the Reynolds number and the gap ratio.

The SOR iterative method is utilized in order to obtain the steady–state solution (the main flow) and also to solve the eigenvalue problem in the linear stability analysis. The steady–state solution is obtained numerically by solving Eqs. (3) and (4) under boundary conditions, where the spatial derivatives are approximated by the second–order finite differences. The antisymmetry of $(\bar{\psi}, \bar{\omega})$ with respect to the x-axis, i.e. $\bar{\psi}(x, -y) = -\bar{\psi}(x, y)$ and $\bar{\omega}(x, -y) = -\bar{\omega}(x, y)$, is taken into consideration in calculating the steady–state solutions in order to save computational time. In the SOR iterative method to solve the eigenvalue problem in the linear stability analysis, the spatial derivatives are approximated by the second–order finite differences. Here, it is added that the eigenfunctions $(\hat{\psi}, \hat{\omega})$ of the most growing mode has the symmetry $\hat{\psi}(x, -y) = \hat{\psi}(x, y)$ and $\hat{\omega}(x, -y) = \hat{\omega}(x, y)$, which can be utilized in numerical calculation.

6. Numerical results

Our numerical simulation was performed in the range of $Re \leq 100$ and $0.3 \leq \Gamma \leq 5.0$, and showed that the flow pattern is categorized into six kinds of flow, i.e. a steady symmetric flow, anti–phase and in–phase oscillatory flows, an oscillatory flow, a deflected oscillatory flow, and a steady asymmetric flow, each of which is depicted in Figs. 3 (a)– 3 (f), respectively. The steady symmetric flow is uniquely realized at Reynolds numbers smaller than a critical Reynolds value Re_c, which is determined depending on Γ.

The first instability is caused by oscillatory disturbances when the gap ratio is very small. For example, we show two flow fields for $\Gamma = 0.5$ at $Re = 40$ and 50 in Figs. 3(a) and 3(b),
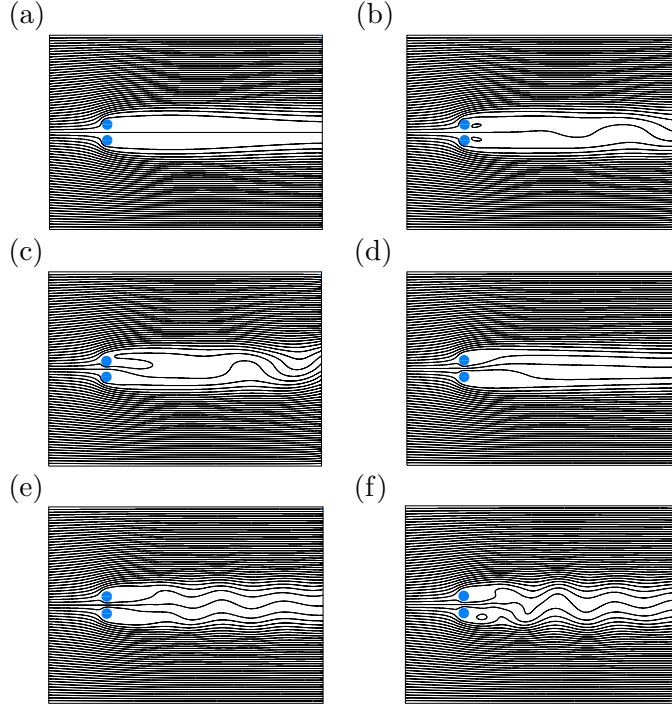
Figure 3. Flow pattern. (a) Steady symmetric flow. $\Gamma = 0.5$, $Re = 40$. (b) Oscillatory flow. $\Gamma = 0.5$, $Re = 50$. (c) Deflected oscillatory flow. $\Gamma = 0.5$, $Re = 60$. (d) Steady asymmetric flow. $\Gamma = 0.6$, $Re = 57$. (e) In-phase synchronously oscillating flow. $\Gamma = 0.62$, $Re = 55$. (f) Deflected oscillatory flow. $\Gamma = 0.62$, $Re = 60$.
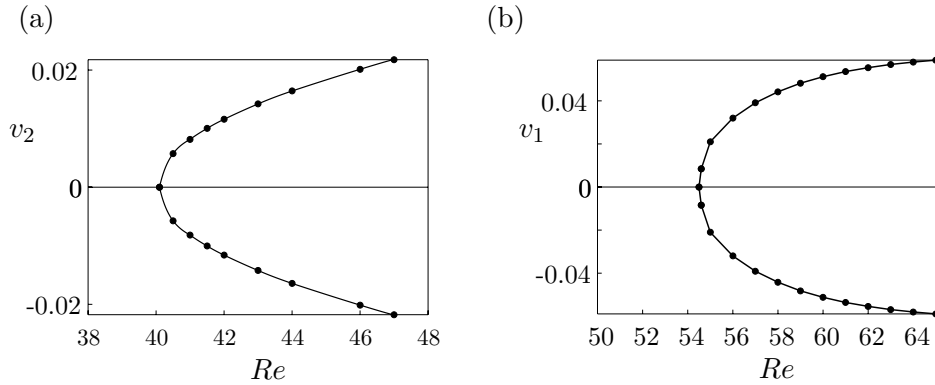
Figure 4. Bifurcation diagram. $\Gamma = 0.5$. (a) Hopf bifurcation. (b) Pitchfork bifurcation.

respectively. The flow is steady and symmetric at $Re = 40$ (Fig. 3 (a)), but oscillatory at $Re = 50$ (Fig. 3(b)). Oscillation in the flow is observed in significantly apart places behind the two cylinders. In order to analyze the transition, we take the amplitude of oscillation of velocity v_2 in the y-direction at the point P_2 in Fig. 1 and draw a bifurcation diagram. The bifurcation diagram thus obtained is shown in Fig. 4(a), where the amplitude (maximum and minimum values, $\overline{v_2}$ and $\underline{v_2}$, in oscillation) of v_2 in periodic oscillation is depicted against Re. From the relation of $|\overline{v_2} - \underline{v_2}| \propto (Re - Re_c)^{1/2}$, the bifurcation is judged to be a Hopf bifurcation with $Re_c = 40.1$. We confirmed a deflected oscillatory flow at $Re = 60$ that was found by Kang[5] as shown in Fig. 3(c). In this figure, the deflection is observed just behind the gap between the
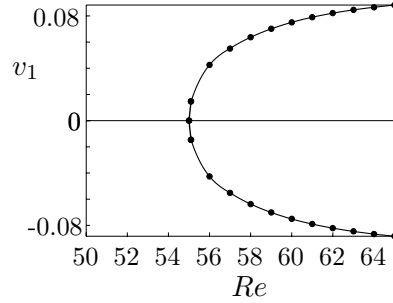
Figure 5. Bifurcation diagram. Pitchfork bifurcation. $\Gamma = 0.6$.

two cylinders, whereas the oscillation occurs far downstream from the cylinders as in Fig. 3(b). In order to examine the flow deflection, we take the velocity v_1 in the y-direction at the point P_1 in Fig. 1, which lies nearer downstream of cylinders than P_2. From the bifurcation diagram shown in Fig. 4(b), a pitchfork bifurcation is confirmed with the critical Reynolds number $Re_c = 54.6$. It is strange that the pitchfork bifurcation occurs at larger Reynolds number than the critical value for the Hopf bifurcation. We conclude that the two different bifurcations occur in separate distinct regions in the whole flow field, whose representative points are P_1 and P_2 for the pitchfork and Hopf bifurcations, respectively.

For a little larger gap ratio, $\Gamma = 0.6$, the flow experiences instability due to a stationary disturbance first as the Reynolds number increases gradually and its bifurcation is a pitchfork bifurcation with $Re_c = 55.1$ as depicted in Fig. 5, which is drawn in the same manner to Fig. 4(b). The resultant flow is a steady asymmetric flow (Fig. 3 (d)). We can see the asymmetry in the wake of the two cylinders, which is an unexpected flow pattern because we usually expect oscillatory flows for the flow past any symmetrically arranged obstacles.

The steady asymmetric flow do not occur for $\Gamma = 0.62$ in numerical simulation. The flow becomes oscillatory first with gradual increase of the Reynolds number. A snapshot of the oscillatory flow field at $Re = 55$ is depicted in Fig. 3(e), in which the wakes behind the cylinders oscillate synchronously in the same phase and oscillation is observed immediately behind the cylinders in contrast with Fig. 3(b) where oscillation occurs far downstream from the cylinders. Taking the velocity v_2 as in Fig. 4(a), we depicted a bifurcation diagram and identified it as a Hopf bifurcation with $Re_c = 54.5$. In addition, a pitchfork bifurcation is confirmed by numerical calculation for the steady solutions and the critical Reynolds number is evaluated as $Re_c = 55.4$. It is noted that such steady flows are not realied in experiment or numerical simulation. However, the influence of pitchfork bifurcation is clearly seen in the flow pattern at $Re = 60$ (Fig. 3 (f)), where deflected oscillatory flow is observed. We show the flow field of the disturbance $\hat{\psi}$ in Figs. 6. It is confirmed that the flow field of disturbance at $Re = 55$ is symmetric with respect to the-x axis (Fig. 6 (c)), but it is asymmetric at $Re = 60$ by the influence of the pitchfork bifurcation (Fig. 6 (d)).

Comparing the flow field of disturbance for $\Gamma = 0.6$ ($Re = 60$, Fig. 6 (b)) with that for $\Gamma = 0.62$ ($Re = 60$, Fig. 6 (d)), we can see that the disturbance for $\Gamma = 0.6$ has a significant magnitude in a restricted region of the whole field, whereas the disturbance extends in the entire flow field for $\Gamma = 0.62$. Hence, we conclude that the two modes of disturbance are different and the most unstable disturbance changes from one mode to the other in a very narrow range $0.6 < \Gamma < 0.62$.

We show the transition diagram in Fig. 7, which is drawn compiling the numerical results for $0.3 \leq \Gamma \leq 1.0$, where the critical Reynolds number for the Hopf bifurcation is indicated by dashed lines with filled circles and the pitchfork bifurcation by solid line with open circles. From this figure, it is seen that the flow can be classified by the first instability into three categories.
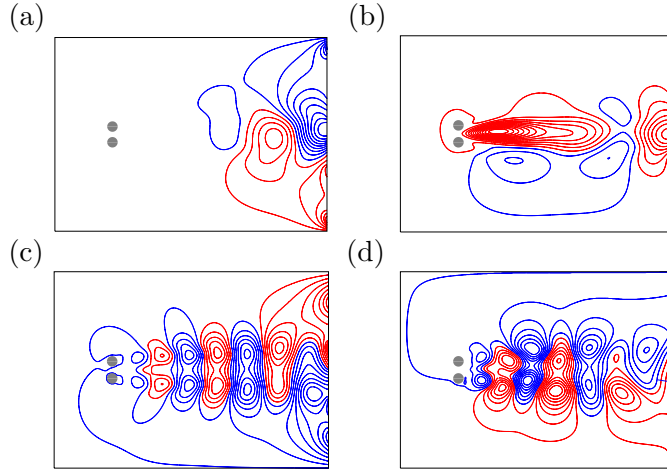
Figure 6. Flow pattern of disturbance. (a) $\Gamma = 0.5$, $Re = 50$, (b) $\Gamma = 0.6$, $Re = 60$. (c) $\Gamma = 0.62$, $Re = 55$. (d) $\Gamma = 0.62$, $Re = 60$.

For $\Gamma < 0.58$, the flow is unstable to an oscillatory disturbance to yield oscillation in a restricted region far downstream and then becomes a deflected oscillatory flow at large Reynolds numbers. For $0.58 < \Gamma < 0.62$, a steady asymmetric flow is realized above a critical Reynolds number and then a deflected oscillatory flow appears. For $0.62 < \Gamma < 1.0$, the flow oscillates in the entire flow field and becomes a deflected oscillatory flow. It is added that there are two different modes of synchronous oscillation in the flow, one of which is oscillation in the same phase observed in the present paper ($\Gamma = 0.62$) and the other is oscillation in the anti-phase. The exchange of the two different synchronous oscillation modes in the flow past two circular cylinders was discussed in our previous paper[7].
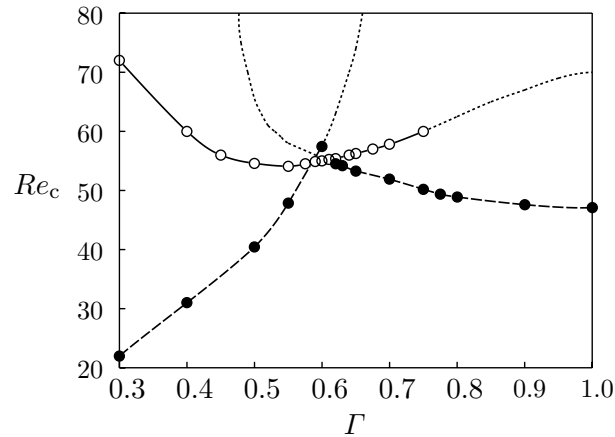
Figure 7. Transition diagram. ○: Pitchfork bifurcation, ●: Hopf bifurcation.

[1] Y. Ohya, A. Okajima and M. Hayashi. "Wake Interference and vortex shedding", *Encyclopedia of Fluid Mechanics* (Ed. N. P. Cheremisinoff, Gulf Pub., Houston), **8** (1988) 323-389.
[2] S. Ishigai, E. Nishikawa, K. Nishimura and K. Cho, "Experimental study on structure of gas flow in tube banks with tube axes normal to flow," *Bull. JSME*, **15** (1972) 949-956.
[3] J. Mizushima and N. Suehiro, "Instability and transition of flow past two tandem circular cylinders", *Phys. Fluids.*, **17** (2005) 104107-104107-11.
[4] C. H. K. Williamson, "Evolution of a single wake behind a pair of bluff bodies", *J. Fluid Mech.*, **159** (1985) 1-18.

[5] S. Kang, "Characteristics of flow over two circular cylindrs in a side-by-side arrangement at low Reynolds numbers", *Phys. Fluids*, **15** (2003) 2468-2498.

[6] L. J. Steger and L. R. Sorenson, "Automatic mesh-point clustering near a boundary in grid generation with elliptic partial differential equation", *J. Comp. Phys.*, **33** (1979) 405-410.

[7] T. Akinaga, J. Mizushima "Linear Stability of Flow past Two Circular Cylinders in a Side-by-side Arrangement", *J. Phys. Soc. Jpn.*, **74** (2005) 1366-1369.